JACC: BASIC TO TRANSLATIONAL SCIENCE VOL. 5, NO. 7, 2020

PRECLINICAL RESEARCH

Paclitaxel Drug-Coated Balloon Angioplasty Suppresses Progression and Inflammation of Experimental Atherosclerosis in Rabbits

Mohammed M. Chowdhury, MB ChB, PhD,[a,d,*] Kanwarpal Singh, PhD,[b,*] Mazen S. Albaghdadi, MD, MSc,[a] Haitham Khraishah, MD,[a,e] Adam Mauskapf, BS,[a] Chase W. Kessinger, PhD,[a] Eric A. Osborn, MD, PhD,[a,e] Stephan Kellnberger, PhD,[a] Zhonglie Piao, PhD,[b] Christian L. Lino Cardenas, PharmD, PhD,[a] Madeleine S. Grau, BA,[a] Michael R. Jaff, DO,[f] Kenneth Rosenfield, MD,[a] Peter Libby, MD,[g] Elazer R. Edelman, MD, PhD,[g,h] Mark E. Lindsay, MD, PhD,[a] Guillermo J. Tearney, MD, PhD,[b,c,†] Farouc A. Jaffer, MD, PhD[a,b,†]

VISUAL ABSTRACT

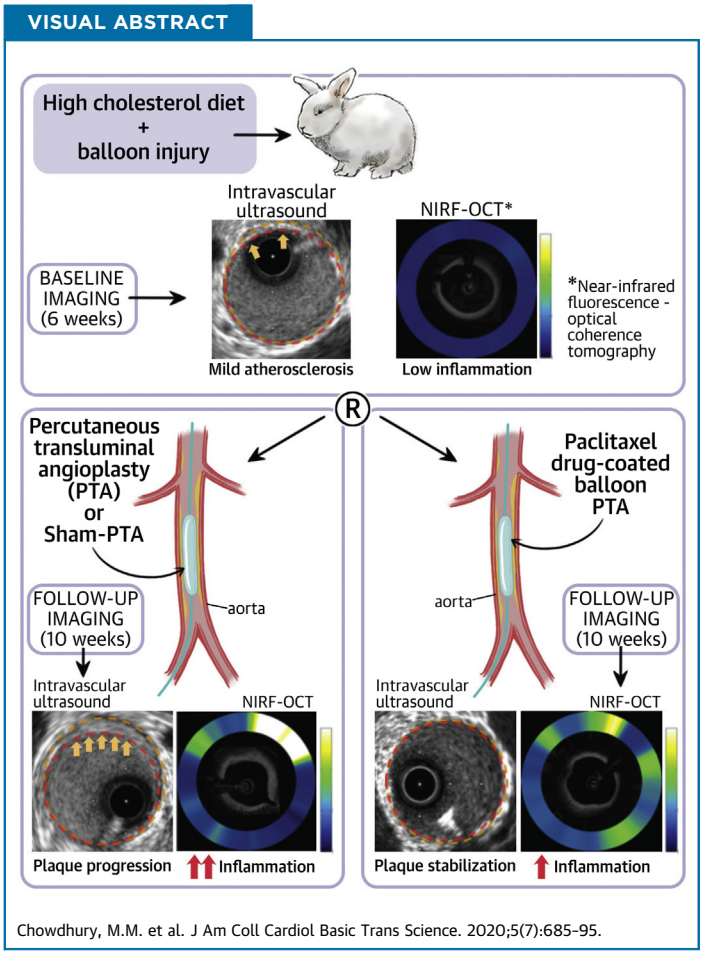

Chowdhury, M.M. et al. J Am Coll Cardiol Basic Trans Science. 2020;5(7):685–95.

From the [a]Cardiovascular Research Center, Division of Cardiology, Massachusetts General Hospital, Harvard Medical School, Boston, Massachusetts; [b]Wellman Center for Photomedicine, Massachusetts General Hospital, Harvard Medical School, Boston, Massachusetts; [c]Department of Pathology, Massachusetts General Hospital, Harvard Medical School, Boston, Massachusetts; [d]Department of Vascular and Endovascular Surgery, Department of Surgery, Addenbrooke's Hospital, University of Cambridge,

ISSN 2452-302X https://doi.org/10.1016/j.jacbts.2020.04.007

ABBREVIATIONS AND ACRONYMS

2D = 2-dimensional

CSA = cross-sectional area

DCB = drug-coated balloon

EEM = external elastic membrane

IVUS = intravascular ultrasound

NIRF = near-infrared fluorescence

OCT = optical coherence tomography

PAD = peripheral arterial disease

PAV = percent atheroma volume

PB = plaque burden

PTA = percutaneous transluminal angioplasty

PTX = paclitaxel

TAV = total atheroma volume

HIGHLIGHTS

- **Restenosis limits the efficacy of PTA or stent treatment of atherosclerosis in peripheral and coronary artery disease.**
- **Paclitaxel DCBs effectively reduce restenosis; however, recently, their overall safety profile has been called into question.**
- **In an in vivo molecular-structural imaging study of 25 rabbits with experimental atherosclerosis, DCB-PTA, plain PTA, or sham-PTA was investigated using serial intravascular NIRF-OCT and IVUS.**
- **DCB-PTA reduced lesion inflammation on NIRF-OCT and halted lesion progression on IVUS, compared with PTA or sham-PTA.**
- **These findings indicated the potential for DCBs to serve effectively and safely as a regional anti-atherosclerosis therapy.**

SUMMARY

Paclitaxel drug-coated balloons (DCBs) reduce restenosis, but their overall safety has recently raised concerns. This study hypothesized that DCBs could lessen inflammation and reduce plaque progression. Using 25 rabbits with cholesterol feeding- and balloon injury-induced lesions, DCB-percutaneous transluminal angioplasty (PTA), plain PTA, or sham-PTA (balloon insertion without inflation) was investigated using serial intravascular near-infrared fluorescence–optical coherence tomography and serial intravascular ultrasound. In these experiments, DCB-PTA reduced inflammation and plaque burden in nonobstructive lesions compared with PTA or sham-PTA. These findings indicated the potential for DCBs to serve safely as regional anti-atherosclerosis therapy. (J Am Coll Cardiol Basic Trans Science 2020;5:685–95)

Cambridge, United Kingdom; [e]Cardiovascular Division, Beth Israel Deaconess Medical Center, Harvard Medical School, Boston, Massachusetts; [f]Department of Medicine, Massachusetts General Hospital, Harvard Medical School, Boston, Massachusetts; [g]Cardiovascular Division, Brigham and Women's Hospital, Harvard Medical School, Boston, Massachusetts; and the [h]Institute for Medical Engineering and Science, Massachusetts Institute of Technology, Cambridge, Massachusetts. *Drs. Chowdhury and Singh contributed equally to this work and are joint first authors. †Drs. Tearney and Jaffer contributed equally to this work and are joint senior authors. Juan Granada, MD, served as Guest Editor for this paper. Dr. Chowdhury is supported by fellowships from the Royal College of Surgeons of England, the British Heart Foundation (BHF; FS/16/29/31957), the University of Cambridge (Parke-Davies Fellowship Award), and the President's Early Career Award from the Circulation Foundation (UK Vascular Charity-awarded to Mr P. Coughlin, Vascular Surgery Department, University of Cambridge). Dr. Jaffer is supported by the National Institutes of Health (NIH) (grants R01 HL122388, R01 HL137913, R01 HL150538) and an MGH Hassenfeld Research Scholar Award. Dr. Osborn is supported by the NIH (grant K08 HL130465). Dr. Kellnberger is supported by an American Heart Association (AHA) postdoctoral fellowship award (17POST33670288). Drs. Cardenas and Lindsay are supported by the Toomey Fund for Aortic Dissection and the Fredman Fellowship. Dr. Libby is supported by the National Heart, Lung, and Blood Institute (R01HL080472), AHA (18CSA34080399), and RRM Charitable Fund. Dr. Edelman was supported in part by a grant from the NIH (R01GM49039). Dr. Albaghdadi has taken part in sponsored research from Kowa, Pfizer, and Sanofi. Dr. Olsen has been a consultant for Abbott Vascular; and has been a member of the scientific advisory board for Dyad Medical. Dr. Jaff has been a noncompensated advisor to Boston Scientific; has been a compensated advisor to Medtronic Vascular, Philips/Volcano, Biotronik, Vactronix, EFemoral, and R3 Vascular; and has been an equity shareholder in Vascular Therapies, EFemoral, and R3 Vascular. Dr. Rosenfield has been a member of the scientific advisory board and a consultant for Abbott Vascular, Access Vascular, Boston Scientific-BTG, Volcano-Philips, Surmodics, Cruzar, Magneto, Micell, Summa Therapeutics, and Thrombolex; holds stocks/stock options in Access Vascular, Accolade, Contego, Endospan, Embolitech, Eximo, JanaCare, PQ Bypass, Primacea, MD Insider, Shockwave, Silk Road, Summa Therapeutics, Cruzar Systems, Capture Vascular, and Magneto; and has been a Board Member for Viva Physicians and National PERT Consortium. Dr. Libby has received research funding in the last 2 years from Novartis; has been an unpaid consultant to, or involved in clinical trials for, Amgen, AstraZeneca, Esperion Therapeutics, Ionis Pharmaceuticals, Kowa Pharmaceuticals, Novartis, Pfizer, Sanofi-Regeneron, and XBiotiech, Inc; and has been a member of scientific advisory board for Amgen, Athera Biotechnologies, Cordivia Therapeutics, DalCor Pharmaceuticals, IFM Therapeutics, Kowa Pharmaceuticals, Olatec Therapuetics, Medimmune, Novartis, and XBiotech, Inc. Dr. Tearney has taken part in sponsored research from VivoLight, Canon, and AstraZeneca; has received royalties and catheter components from Terumo; and has a financial/fiduciary interest and consults for SpectraWAVE, a company developing an OCT-NIRS intracoronary imaging system and catheter. Dr. Jaffer has taken part in sponsored research from Canon and Siemens; has been a consultant for Boston Scientific, Abbott Vascular, Siemens, Biotronik, Philips, and Acrostak; and holds equity interest in Intravascular Imaging, Inc. Drs. Tearney and Jaffer have received royalties for Terumo, Canon, and Spectrawave for a patent pending with Massachusetts General Hospital.
The authors attest they are in compliance with human studies committees and animal welfare regulations of the authors' institutions and Food and Drug Administration guidelines, including patient consent where appropriate. For more information, visit the *JACC: Basic to Translational Science* author instructions page.

Manuscript received February 12, 2020; revised manuscript received April 13, 2020, accepted April 13, 2020.

Compared with percutaneous transluminal angioplasty (PTA) using standard balloons, paclitaxel (PTX)–eluting, drug-coated balloons (DCBs) have recently shown improved efficacy in treating peripheral arterial disease (PAD)– or coronary artery disease–based restenosis and have become the primary endovascular treatment for femoropopliteal PAD (1-5). However, at present, scant data exist regarding the effects of DCB-PTA on atherosclerosis progression in vivo or the mechanisms by which it may produce its biological effects on atheroma in vivo. A recent meta-analysis of randomized trials demonstrated the potential for paclitaxel DCBs to increase all-cause mortality (6,7); in contrast, several other PTX DCB studies have not shown any differences in overall mortality (8-10). Therefore, additional studies investigating the effects of PTX DCBs on atherosclerosis could provide greater understanding of their vascular safety profile.

This study evaluated the effects of PTX DCB-PTA on inflammation and lesion progression in rabbit atherosclerosis in vivo and compared the results to animals treated with conventional PTA or sham-PTA. In addition to assessing plaque atheroma volume and plaque burden (PB) changes by serial intravascular ultrasound (IVUS), we assessed changes in lesion inflammation using serial intravascular near-infrared fluorescence–optical coherence tomography (NIRF-OCT) molecular–structural imaging of inflammatory protease activity (11,12). To further elucidate mechanisms underlying our in vivo findings, we performed histological and molecular assays of resected lesions and investigated the effects of PTX on human aortic smooth muscle cells in vitro.

METHODS

STUDY DESIGN. All animal studies were approved by the Institutional Animal Care and Use Committee of Massachusetts General Hospital (Protocol #2013N000015). **Figure 1** shows the overview of the in vivo serial imaging study of rabbit atherosclerosis progression and DCB intervention or control subjects.

EXPERIMENTAL ATHEROSCLEROSIS LESION GENERATION. Lesions were generated in rabbit aortas using balloon injury in cholesterol-fed animals (**Figure 1**) as previously performed (13,14). After baseline, 6-week survival intravascular NIRF-OCT, and IVUS imaging, rabbits randomly received 1 of 3 treatments: PTX DCB-PTA (n = 10; IN.PACT Admiral 4.0 × 40 mm, Medtronic, Santa Rosa, California; 3.5 μg/mm^2 of drug-coated concentration with urea excipient); conventional PTA (n = 10; INVATEC Admiral Xtreme 4.0 × 40 mm, Medtronic); or sham-PTA (n = 5), followed by imaging. Animals were sacrificed 4 weeks later at week 10 (Supplemental Appendix).

In brief, atherosclerosis was induced in the aortas of male and female New Zealand White rabbits (aorta diameter: 3 to 3.5 mm; weight: 3 to 4 kg; Charles River Laboratories; Wilmington, Massachusetts) by local balloon arterial injury and high-cholesterol diet. After a 2-week, lead-in atherogenic diet (1% cholesterol, 5% peanut oil, Research Diets, New Brunswick, New Jersey), the infrarenal abdominal aorta of rabbits underwent balloon injury at week 2, as demonstrated previously (1).

INTRAVASCULAR IMAGING OF PB AND PLAQUE INFLAMMATION. IVUS. IVUS images of the abdominal aorta were acquired with a 40-MHz clinical catheter by automated 0.5-mm/s pull back (iLab2, Polaris2 Software Imaging System, Boston Scientific, Marlborough, Massachusetts). Imaging commenced from the abdominal aorta at the level of the lowest renal down to the common iliac artery. IVUS was performed at 6 weeks both pre- and post-angioplasty and at the terminal 10-week imaging session.

IVUS IMAGING QUANTITATIVE ANALYSIS. IVUS datasets at 6 and 10 weeks were manually co-registered to each other using fiducial landmarks, including side branches and the known pull back rates of the imaging systems, and then analyzed by manual segmentation (OsiriX, Geneva, Switzerland; and Fiji imaging v2.0.0, National Institute of Health, University of Wisconsin, Madison, Wisconsin) (15), in accordance with expert consensus IVUS recommendations (16). The cross-sectional area (CSA) of the external elastic membrane (EEM) and vessel lumen were measured every 0.4 mm from axial IVUS images for each rabbit at 6 and 10 weeks, across the area that had undergone balloon treatment (total 40 mm length, 200 images per animal [100 images per timepoint]). These measurements permitted calculation of the atheroma CSA and PB) for each IVUS slice. All obtained cross-sectional slices were analyzed and included in the image analysis results. On a per-slice basis (every 0.4 mm), atheroma progression was quantified as the change in IVUS PB (ΔPB) between 6 and 10 weeks. The Supplemental Appendix section provides the formulas used for NIRF and IVUS quantitative analysis.

NIRF plaque inflammation measurements. Twenty-four hours before NIRF-OCT imaging sessions, rabbits received the protease NIRF imaging agent ProSense750 VM110 intravenously (a quenched sensor engineered to generate fluorescence following proteolytic activation by cathepsins B, L, or S; PerkinElmer, Waltham, Massachusetts) (11). Automated reconstruction of dual-modal NIRF-OCT pull backs

FIGURE 1 Experimental Study Design

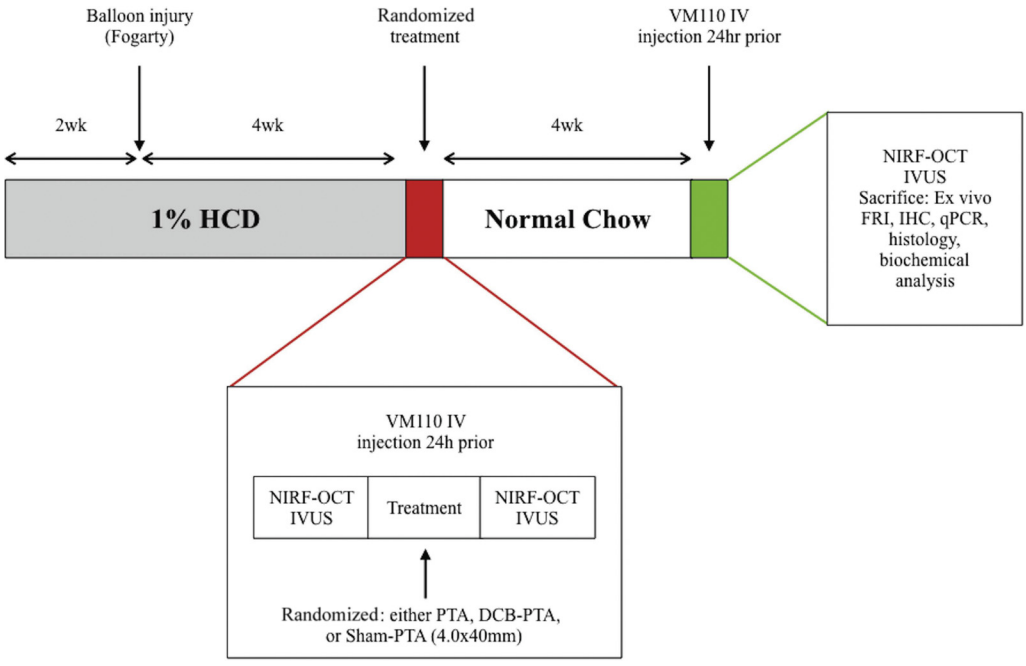

All 25 rabbits received 1.0% high-cholesterol diet (HCD) 2 weeks before aorta balloon injury, and for 4 weeks thereafter, followed by normal chow for the final 4 weeks. At 4 weeks after balloon injury, rabbits were intravenously injected with ProSense VM110 (400 nmol/kg). Rabbits underwent in vivo multimodal survival near-infrared fluorescence–optical coherence tomography (NIRF-OCT), intravascular ultrasound (IVUS), and x-ray angiography 24 h later. Then animals randomly underwent drug-coated balloon percutaneous transluminal angioplasty (DCB-PTA) (n = 10), PTA (n = 10), or sham-PTA (n = 5) therapy. Four weeks later at week 10, multimodal imaging NIRF-OCT and IVUS imaging were repeated, followed by sacrificed and ex vivo fluorescence imaging, as well as RNA and histopathological analysis. FRI = fluorescence reflectance imaging; IHC = immunohistochemistry; qPCR= quantitative polymerase chain reaction.

was performed, as previously described (17). Quantitative NIRF data were generated using co-registered OCT images to correct the NIRF signal according to the distance between the catheter and the lumen surface, and expressed as both the NIRF concentration (nM) averaged over all the slices that included the plaque and the average NIRF concentration per OCT slice at 0.4 mm intervals (11). The change in NIRF concentration (ΔNIRF, in nM) on a per slice basis was calculated as the difference between the NIRF concentration at 6 and 10 weeks.

Readers (M.M.C., K.S., M.S.A.) were blinded to the group assignment of each animal for all IVUS and NIRF image analyses.

MOLECULAR ANALYSIS. Following sacrifice, rabbit aortas were perfused with cold saline and harvested. Aortas were then processed, measured, and sectioned. Sections were created every 0.5 cm, with selected tissue from 3 regions stored in RNAlater for subsequent RNA analysis. The 3 regions included: 1) the normal aorta (no Fogarty balloon injury); 2) the PTA segment (Fogarty balloon injured and then staged experimental angioplasty 4 weeks later) (Figure 1); and 3) the balloon-injured region (Fogarty balloon injury only). The remaining tissue was snap frozen using dry ice and 2-methylbutane, then placed in optimal cutting temperature compound medium and stored at −80 °C for later sectioning and histopathology.

IN VITRO STUDIES. Primary human smooth muscle cells from healthy donors were purchased from Cell Applications Inc (Cat #354K-05a, San Diego, California). Human smooth muscle cells were incubated with lipopolysaccharide 100 ng/ml in vitro for 24 h and then incubated with graded concentrations of PTX up to 1×10^{-5} M for 90 min. Cells then underwent RNA extraction and quantitative polymerase chain reaction analysis as detailed in the Supplemental Appendix.

STATISTICAL ANALYSIS AND REPRODUCIBILITY. Continuous variables were reported mean ± SD,

FIGURE 2 Representative NIRF Inflammation and IVUS Plaque Burden Imaging of DCB-PTA, PTA, and Sham-PTA Groups

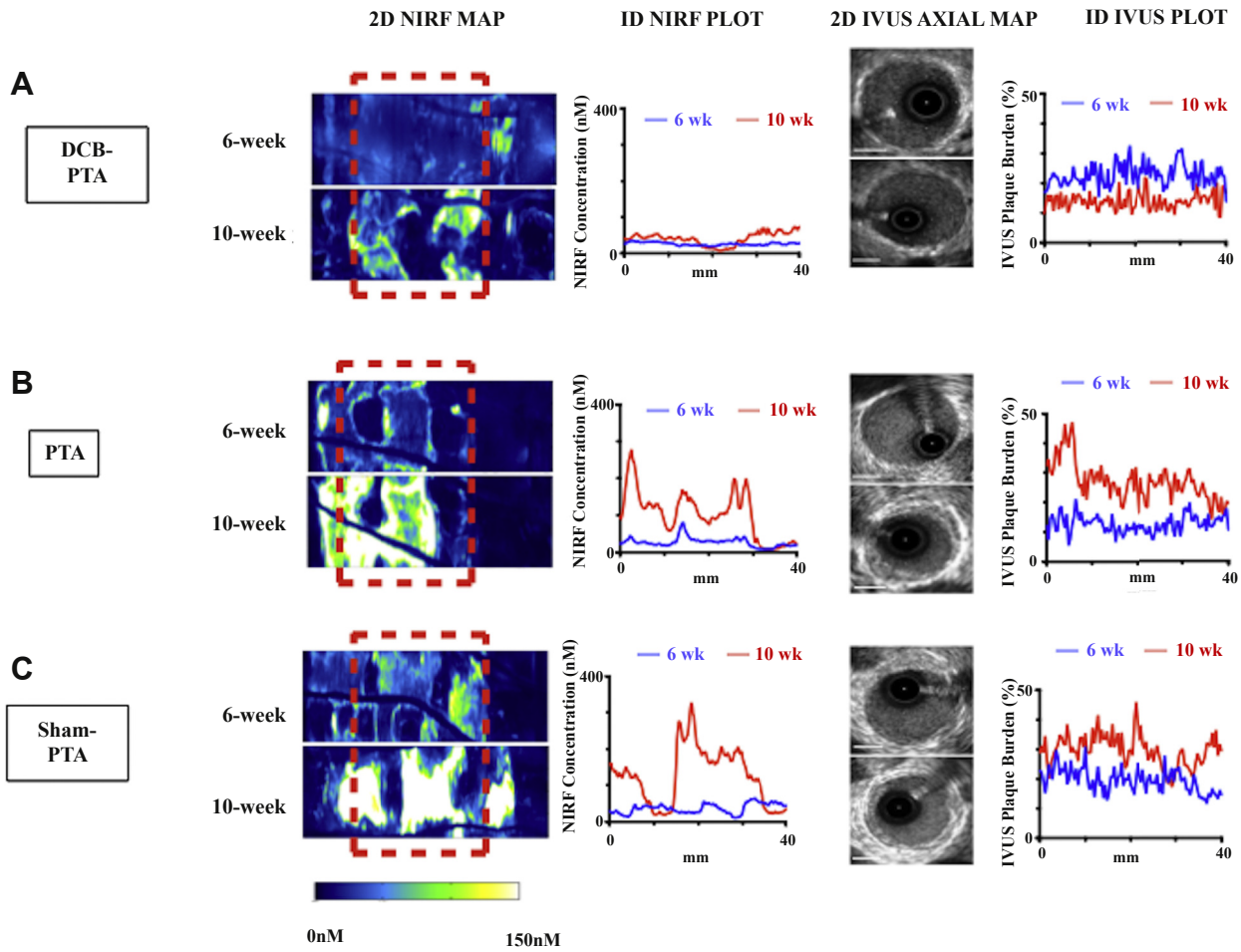

Depiction of 2D NIRF maps at 6-week and 10-week timepoints after injection (24 h prior) with ProSense VM110, comparing **(A)** DCB-PTA, **(B)** PTA, and **(C)** Sham-PTA representative subjects. The area subject to angioplasty is illustrated by the **red dotted box** (2D NIRF map). The accompanying 1D plots show the NIRF concentration and plaque burden by IVUS at both timepoints. Inset graphs demonstrate 6-week **(blue)** and 10-week **(red)** keys. IVUS **white scale bar**, 1 mm. Complete intravascular imaging data is presented in Supplemental Figures S1 to S3. 2D = 2-dimensional; 1D = 1-dimensional; other Abbreviations as in **Figure 1**.

median (25th, 75th percentiles), or median interquartile range (IQR), as appropriate. Normality was assessed visually using histograms and Q-Q plots, and formally using the Shapiro-Wilk test. The nonparametric Kruskal-Wallis test compared the differences among DCB-PTA, PTA, and sham-PTA groups, and the Mann Whitney U test compared differences between DCB-PTA and PTA groups. Regression analyses using simple and multiple linear regression models were adjusted for baseline (week 6) serum cholesterol, C-reactive protein, minimum lumen area, and the respective plaque parameters (baseline percent atheroma volume [PAV], total atheroma volume [TAV], and PB). For each model, formal statistical tests of the linear regression assumptions were performed. A log-transformation to the ΔNIRF as an outcome variable was performed to improve the model fit. Findings are reported as a percentage change derived from geometric mean ratios. For all regression experiments, sensitivity analyses were performed using serum cholesterol and C-reactive protein levels at endpoint (week 10), instead of baseline. We also examined correlations between ΔNIRF and other IVUS-derived metrics using Pearson's correlation. For histological and mRNA analyses, comparisons between groups were made using the Kruskal-Wallis H test, with a post hoc analysis using Dunn's test of multiple comparisons. The p values were

TABLE 1 Lesion Anatomical and Inflammation Measures, and Cholesterol and CRP Levels for DCB-PTA, PTA, and Sham-PTA Groups

	DCB-PTA (n = 10)	PTA (n = 10)	Sham-PTA (n = 5)	p Value
Total atheroma volume (mm^3)				
6 weeks	165.6 (31.0)	145.6 (21.7)	137.0 (16.4)	0.348
10 weeks	142.1 (45.1)	237.5 (32.0)	302.8 (164.3)	<0.001*
Δ Change	−19.7 (4.6)	98.0 (64.7)	183.6 (155.5)	<0.001*
Percent atheroma volume (%)				
6 weeks	16.0 (4.4)	14.3 (5.1)	12.8 (5.1)	0.136
10 weeks	14.0 (4.3)	21.1 (3.7)	19.5 (6.6)	0.001†
Δ Change	−3.0 (4.6)	5.7 (4.1)	9.6 (1.4)	0.001†
Average plaque burden (%)				
6 weeks	16.2 (5.5)	14.2 (4.9)	12.9 (5.2)	0.179
10 weeks	14.6 (5.3)	19.9 (4.2)	19.7 (6.3)	0.009†
Δ Change	-2.5 (7.6)	5.8 (4.0)	9.8 (1.0)	0.004†
Minimal lumen area (mm^2)				
6 weeks	5.5 (2.1)	6.3 (1.9)	6.6 (1.7)	0.600
10 weeks	7.0 (1.3)	7.9 (1.9)	7.5 (3.0)	0.379
Δ Change	1.1 (3.1)	0.7 (2.0)	2.6 (3.9)	0.944
Percent area stenosis, average (%)				
6 weeks	26.9 (6.9)	23.4 (4.5)	27.6 (9.1)	0.417
10 weeks	21.1 (5.6)	21.9 (7.4)	27.6 (10.4)	0.392
Δ Change	−5.2 (4.0)	−1.2 (2.1)	0.0 (0.5)	<0.001*
NIRF inflammation, average (nM)				
6 weeks	17.8 (10.2)	19.6 (3.9)	17.6 (10.1)	0.818
10 weeks	40.2 (43.5)	63.4 (45.7)	63.5 (57.9)	0.092
Δ Change	18.3 (43.8)	44.6 (35.5)	48.4 (47.6)	0.100
Total cholesterol (mg/dl)				
6 weeks	1,654.0 (691.0)	2,153.0 (867.0)	1,967.0 (79.0)	0.304
10 weeks	439.5 (310.0)	572.5 (634.0)	214.0 (133.0)	0.051
Δ Change	−1,082.0 (382.0)	−1,620.0 (759.0)	−1,668.0 (756.0)	0.394
CRP (ng/ml)				
6 weeks	19.4 (8.0)	26.8 (12.6)	9.6 (6.4)	0.017‡
10 weeks	22.7 (29.7)	24.6 (51.9)	10.5 (7.7)	0.038‡
Δ Change	−0.4 (31.1)	1.7 (6.6)	−1.7 (6.3)	0.650

Values are median (interquartile range). Plaque area measurement obtained using intravascular ultrasound (IVUS). All 6-week imaging measures were obtained from IVUS or near-infrared fluorescence-optical coherence tomography (NIRF-OCT) images collected before drug-coated balloon percutaneous transluminal angioplasty (DCB-PTA), PTA, or sham-PTA. *p < 0.001; †p < 0.01; ‡p < 0.05.

CRP = C-reactive protein.

2-sided, and a p value of <0.05 was considered statistically significant. Analyses were performed using Stata/IC version 15.0 (StataCorp, College Station, Texas).

For the purposes of direct statistical analysis, comparative data were analyzed between the DCB-PTA and PTA groups, specifically with reference to regression analyses. Sham-PTA data are available in the Supplemental Appendix.

RESULTS

A total of 25 rabbits with aortic lesions (15 male, 10 female) were randomized in the study (**Figure 1**), with 10 receiving PTX DCB-PTA, 10 receiving uncoated PTA, and 5 rabbits receiving sham-PTA. All animals survived until the planned sacrifice at 10 weeks and entered the analysis.

Serial IVUS images of lesion anatomy and NIRF-OCT images of inflammatory cathepsin protease activity were acquired for all 3 groups, with representative 2-dimensional (2D) NIRF maps, 1D NIRF plots, 2D IVUS images, and 1D IVUS plots (**Figure 2**). Complete rabbit data showcasing 2D NIRF maps, quantitative 1D plots, and corresponding 1D IVUS PB plots are presented in Supplemental Figures S1 to S3.

EFFECTS OF DCB-PTA, PTA, OR SHAM-PTA OF ATHEROSCLEROSIS BURDEN AND INFLAMMATION. In all rabbits at both 6 and 10 weeks, IVUS frames were analyzed every 0.4 mm over each 40 mm angioplasty balloon length (100 image slices per rabbit per time point; a total of 5,000 IVUS images underwent assessment of lesion plaque area, lumen area, and vessel wall area). The total lesion plaque volume and burden was calculated over the angioplasty region for each rabbit. The baseline 6-week, follow-up 10 week, and change in plaque characteristics, cholesterol, and C-reactive protein measurements are presented in **Table 1**. At the week 6 baseline, the 3 groups exhibited similar plaque structural measures, including PAV, TAV, and PB (p = 0.348, p = 0.136, and p = 0.179, respectively). Similarly, the 3 groups had comparable baseline NIRF lesion inflammation (**Table 1**) (p = 0.818). The average percentage area stenosis for each group (DCB-PTA, PTA, and sham-PTA) was 20.8%, 22.1%, and 24.8%, respectively, which indicated the presence of mildly stenotic plaques at baseline 6-week imaging.

At follow-up assessment at 10 weeks (4 weeks after baseline imaging), DCB-PTA induced several benefits on experimental lesions, in comparison to the PTA and sham-PTA groups (**Table 1**). Analyzing changes in lesion anatomical features, DCB-PTA significantly reduced lesion progression, and moreover, induced lesion regression (DCB-PTA, PTA, sham-PTA, respectively): AV (−19.7 mm^3 [4.6], 98.0 mm^3 [64.7], 183.6mm^3 [155.5]; p < 0.001); DPAV (−3.0% [4.6], 5.7% [4.1], 9.6% [1.4]; p = 0.001); D average PB (−2.5% [7.6], 5.8% [4.0], 9.8% [1.0]; p = 0.004). DCB-PTA also significantly reduced lesion percent area stenosis by 5.2% (p < 0.001 vs. the other groups). The minimal luminal area also increased over time in all groups. In addition, DCB-PTA significantly reduced the progression of lesion inflammation compared with the PTA group (average NIRF cathepsin activity: 18.3 nM [43.8] vs. 44.6 nM [35.5]; p=0.028) (Supplemental Table 1).

TABLE 2 Assessment of DCB-PTA Versus PTA on Plaque Progression

	DCB-PTA vs. PTA (Unadjusted)			DCB-PTA vs. PTA (*Adjusted)		
	Estimate	95% Confidence Intervals	p Value	Estimate	95% Confidence Intervals	p Value
Δ Total atheroma volume (mm^3)	−1,14.5	−152.4 to −76.6	<0.001†	−114.0	−159.6 to −68.4	<0.001†
Δ Percent atheroma volume (%)	−8.5	−12.7 to −4.4	<0.001†	−8.2	−11.7 to −4.7	<0.001†
Δ Average plaque burden (%)	−7.3	−12.1 to −2.5	0.005‡	−7.0	−11.6 to −2.4	0.006‡

Unadjusted and adjusted estimates comparing the changes in total atheroma value, percent atheroma value and plaque burden in DCB-PTA vs. PTA (measured as Δ change) derived from generalized linear regression models with 95% confidence intervals. *Adjusted for baseline cholesterol, C-reactive protein, and minimal lumen area, and corresponding atheroma parameter at baseline (6 weeks). †$p < 0.001$; ‡$p < 0.01$.

Abbreviations as in Table 1.

On multivariable analyses adjusted for baseline cholesterol levels, C-reactive protein, minimal lumen area, and baseline IVUS parameters (TAV, PAV, and PB), DCB-PTA remained significantly more effective in reducing TAV, PAV, and average PB compared with PTA, in which all 3 measures increased ($p < 0.006$ for each comparison) (Table 2). Similarly, after adjustment for baseline cholesterol level, C-reactive protein level, minimal lumen area, and baseline NIRF inflammation, treatment with DCB-PTA significantly reduced the average plaque NIRF inflammatory cathepsin activity signal by 48.1% (95% confidence interval: −69.45 to −12.0; $p = 0.018$) (Table 3) compared with the PTA group.

For all regression models, sensitivity analyses using endpoint week 10 levels of C-reactive protein, cholesterol, and minimum lumen area produced the same inference (statistical files in Supplemental Appendix).

RELATIONSHIP BETWEEN PLAQUE INFLAMMATION AND PB OVER TIME. To further assess the relationship between changes in lesion inflammation and changes in PB after angioplasty, we examined the association between the change in NIRF concentration and change in IVUS measures of lesion for each slice by pooling data for both angioplasty groups (DCB-PTA plus PTA groups). Across all pooled slices, the ΔNIRF lesion inflammation correlated positively with ΔTAV, ΔPAV, and ΔPB ($r = 0.50$, $r = 0.49$, and $r = 0.46$, respectively; $p = 0.02$; $p = 0.03$, and $p = 0.04$, respectively) (Table 3) from week 6 to week 10.

EFFECTS OF DCB-PTA, PTA, AND SHAM-PTA ON PLAQUE MACROPHAGE AND SMOOTH MUSCLE CELL CONTENT, AND RNA TRANSCRIPTS IN VIVO AND IN VITRO. To gain mechanistic insight into the effects of PTX on the artery wall, a subgroup of rabbit lesions from PTX DCB-PTA, PTA, and sham-PTA animals underwent histopathological assessment after the week 10 sacrifice. The presence of lesional macrophages (Figure 3A) supported findings that lesions reproduced a key feature of inflammatory atherosclerosis rather than homogeneous smooth muscle cell–rich neointimal hyperplasia characteristic of typical stent restenosis. Following immunohistochemical staining with the RAM-11 rabbit macrophage marker, and the smooth muscle cell smooth muscle actin marker, DCB-PTA–treated lesion sections displayed significantly lower RAM11+ macrophage and smooth muscle actin marker+ area than PTA- or sham-PTA-treated regions (45 to 50 sections analyzed per group for RAM11; $p < 0.001$ [Figures 3A and 3B], and 25 to 30 sections analyzed per group for smooth muscle actin; $p < 0.001$ [Figures 3C and 3D]).

To investigate the effects of DCB-PTA on RNA transcripts, a subgroup of resected aortic lesions from every rabbit underwent RNA extraction and quantification of cathepsin subtype (B, L, S), along with tumor necrosis factor–α and interleukin-1β gene expression. Lesions treated with DCB-PTA exhibited significantly reduced expression of all measured transcripts ($p < 0.001$) compared with lesions from the PTA and sham-PTA groups, which corroborated

TABLE 3 Assessment of DCB-PTA Versus PTA on NIRF Plaque Inflammation, and Relationships Between Plaque NIRF Inflammation and Plaque Progression

Unadjusted and Adjusted Regression Estimates Comparing the Percentage Change Difference in Δ NIRF inflammation Between DCB-PTA vs. PTA (measured as Δ change)		
	% Change (95% CI)	p Value
Δ NIRF (unadjusted)	−52.4 (−72.7 to −16.1)	0.013†
Δ NIRF (*adjusted)	−48.1 (−69.4 to −12.0)	0.018†
Pearson Correlation Coefficients for Δ NIRF vs. IVUS-Derived Metrics (measured as Δ)		
	rp Value	p Value
Δ NIRF vs. Δ TAV	0.50	0.006‡
Δ NIRF vs. Δ PAV	0.49	0.030†
Δ NIRF vs. Δ PB	0.46	0.041†

*Adjusted for baseline cholesterol, baseline CRP, baseline minimal lumen area, and corresponding atheroma parameter, at baseline (6 weeks). †$p < 0.05$; ‡$p < 0.01$.

CI = confidence interval; IVUS = intravascular ultrasound; PAV = percent atheroma volume; PB = plaque burden; rp = reflecting Pearson; TAV = total atheroma volume; other abbreviations as in Table 1.

FIGURE 3 Comparison of Atheroma Macrophage and Smooth Muscle Cell Presence, and Plaque Cathepsin RNA Expression in DCB-PTA, PTA, and Sham-PTA Subjects, as Well as in Vitro Assessment of the Effects of Paclitaxel on Cathepsin Expression in Human Aortic Smooth Muscle Cells

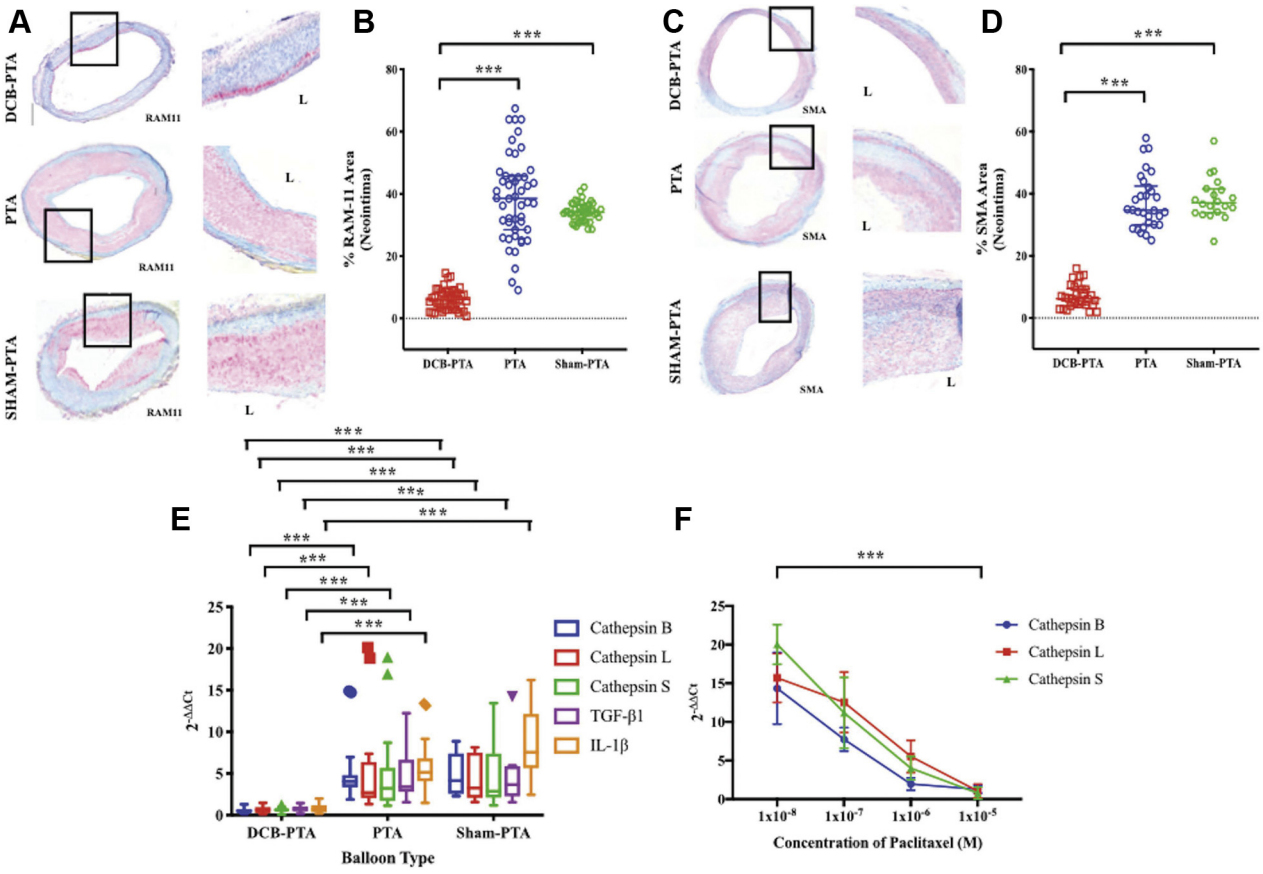

Lesion sections from representative DCB-PTA, PTA, and sham-PTA animals underwent **(A and B)** RAM-11 macrophage (n = 143 sections) and **(C and D)** alpha-actin smooth muscle cell (n = 79 sections) immunohistochemical detection. The percent positively stained area in lesions was assessed; **balloon dots** are actual values per section; **bars** demonstrate median (25th and 75th percentiles). **(E)** Gene expression normalized to the expression of glyceraldehyde 3-phosphate dehydrogenase (GAPDH) (housekeeping gene), displayed using comparative Ct method ($2^{-\Delta\Delta Ct}$). mRNA expression of cathepsin genes measured by quantitative polymerase chain reaction. Verification of expression demonstrated by immunoblotting of cathepsin B, after protein extraction. Statistical comparisons made using Kruskal-Wallis H test, with a post hoc analysis using Dunn's test of multiple comparisons. **(F)** In vitro human aortic smooth muscle cells were incubated with graded concentrations of paclitaxel, and then underwent RNA extraction to assess cathepsin transcripts. n = 4, **bars** demonstrate median (25th and 75th percentiles). ***$p < 0.001$. Abbreviations as in Figure 1.

in vivo findings that showed dampened inflammation following DCB-PTA (Figure 3E).

PTX-BASED EFFECTS ON CATHEPSIN PROTEASE TRANSCRIPT EXPRESSION IN VITRO. To ascertain whether the PTX resident in DCBs could directly exert anti-inflammatory effects relevant to diminished atheroma progression, primary human aortic smooth muscle cells were stimulated with lipopolysaccharide in vitro, and then incubated with graded concentrations of PTX for 90 min. Cells were then processed for mRNA analysis (quantitative polymerase chain reaction; see the Supplemental Appendix). PTX reduced expression of cathepsins B, L, and S mRNA transcripts in aortic smooth muscle cells, in graded fashion ($p < 0.001$) (Figure 3F).

DISCUSSION

Treatment with PTX DCB-PTA, but not conventional PTA or sham-PTA, reduced both lesion inflammation and lesion progression in experimental atherosclerosis in rabbits. These findings provided new experimental evidence that PTX-based DCB treatment favorably affected experimental atherosclerosis, which would have implications for the safety of DCBs,

as well as the ability of DCBs to serve as a regional endovascular therapy for atherosclerosis.

Inflammation drives atherosclerosis progression (18), and anti–interleukin-1β mediated suppression of inflammation can reduce cardiovascular events in patients (19). The present serial intravascular in vivo NIRF-OCT molecular imaging study revealed that DCB-PTA significantly reduced inflammatory protease activity implicated in lesion progression compared with PTA or sham-PTA, in experimental atherosclerosis (20). Macrophages and smooth muscle cells and their products, including cathepsin proteases, contribute to the initiation, progression, and complications of atherosclerosis (21). PTX treatment of human primary aortic smooth muscle cells further demonstrated a dose-dependent reduction in cathepsin mRNA transcripts. The present findings indicated that PTX exerted anti-inflammatory effects that underlay the observed favorable PTX DCB-PTA effects on experimental atherosclerosis.

From a lesional volume perspective, PTX DCB therapy induced experimental lesion regression (decreases in TAV, PAV, average PB, and percent area stenosis) (**Table 1**) in contrast to PTA or sham-PTA treatment. Mechanisms underlying this observation likely include PTX-based anti-inflammatory effects as supported by a moderate correlation between lesion inflammation and lesions progression in these experiments (**Table 3**). Additional mechanisms might include favorable remodeling effects of the balloon angioplasty itself independent of PTX, because the PTA alone group also exhibited reduced lesion progression compared with the sham-PTA group. For example, treatment of experimental atherosclerosis with bare metal stents stabilized rabbit plaques by reducing macrophage content (22,23).

Although the present rabbit model of atherosclerosis (13,14) included a component of restenosis pathology following endovascular injury, the experimental pathology recapitulated several features of human atherosclerosis, such as the presence of plaque macrophages (**Figure 3**). Moreover, although other animal endovascular studies of PTX clearly demonstrated inhibition of neointimal proliferation after balloon injury (24–26), the present study provided new insights into the effects of DCBs on experimental lesions with features of atherosclerosis, which demonstrated inhibition of both lesion inflammation and lesion progression.

The ability to image inflammation in coronary and peripheral artery–sized vessels using high-resolution intravascular NIRF molecular imaging offers a translational approach to understanding the mechanisms of clinical atherosclerosis progression and impaired stent healing (11,12,27,28). A recent first-in-human clinical study in patients with coronary artery disease demonstrated the safety and feasibility of intracoronary NIRF-OCT imaging to detect coronary plaque 633-nm–excited NIR autofluorescence, a potential measure of intraplaque hemorrhage or oxidative stress–induced lipid byproducts (29). The present study thus provided a clinical foundation for NIRF inflammation imaging using ProSense VM110 (Perkin Elmer, Waltham, Massachusetts) (VM110 in Detection of Microscopic Tumors: A Phase I Study; NCT03286062) or LUM015 (Lumicell, Inc., Wellesley, Massachusetts), a similar NIRF cathepsin protease–sensitive agent (30), which were recently evaluated in patients. Both NIRF-OCT catheter technology and imaging agents are positioned to enable clinical NIRF inflammation imaging trials of patients with atherosclerosis in the near future.

This study provided new experimental evidence that PTX DCB-PTA could mitigate lesion inflammation and progression and could therefore serve safely as a regional strategy for treating atherosclerosis. Potential clinical extensions of DCB-PTA could consider treatment of flanking atheroma around culprit plaques in patients already undergoing coronary or peripheral endovascular treatment. However, before extending the application of PTX-DCBs, the current controversy surrounding PTX-DCBs (6–10) requires resolution; the endovascular community eagerly awaits further analyses and new clinical and experimental data. Recent data on the late mortality signal with DCBs remain inconclusive; however, the long-term risks of these devices need to be balanced against their established and sustained efficacy in improving limb-related outcomes in patient with femoropopliteal PAD.

STUDY LIMITATIONS. Balloon injury and severe hyperlipidemia to induce experimental atherosclerosis in rabbits does not fully recapitulate human atherosclerosis complexity but does reproduce some pathological features of human plaques. In addition, the model we used enabled the study of DCBs in atherosclerosis in arteries of a similar caliber to human coronary and peripheral-sized vessels. Furthermore, the investigated experimental lesions induced by balloon injury in this study did not fully recapitulate human atherosclerosis, and therefore, additional DCB studies in clinical subjects are required. A future area of investigation regarding the durability of DCB treatment for preventing atheroma progression in more advanced lesions and for the longer term are questions that exceeded the model and scope of this study. Although the present study required 2 intravascular imaging approaches (NIRF-OCT and

IVUS), further development of an integrated NIRF-IVUS (28) imaging system might provide a single intravascular imaging approach for future atherosclerosis studies.

CONCLUSIONS

PTX DCB-PTA reduced lesion inflammation and lesion progression in experimental rabbit atherosclerosis in contrast to PTA or sham-PTA. These preclinical findings supported the vascular safety and efficacy of PTX-DCB angioplasty.

ACKNOWLEDGMENT The authors thank Dr. Amy Mikkola, MGH Comparative Medicine Clinical Pathology Laboratory, for assay of serum cholesterol levels.

ADDRESS FOR CORRESPONDENCE: Dr. Farouc Jaffer or Dr. Gary Tearney, Massachusetts General Hospital, Cardiovascular Research Center, Simches Research Building, Room 3206, Boston, Massachusetts 02114. E-mail: fjaffer@mgh.harvard.edu OR tearney@mgh.harvard.edu.

PERSPECTIVES

COMPETENCY IN MEDICAL KNOWLEDGE: PTX DCBs reduce peripheral and coronary artery restenosis, but their effects on atherosclerosis have not been fully characterized. There is recent concern regarding their safety profile.

TRANSLATIONAL OUTLOOK 1: PTX DCB-PTA reduces preclinical lesion inflammation and lesion progression in contrast to PTA or sham-PTA, as demonstrated in vivo using translatable intravascular molecular–structural imaging technology.

TRANSLATIONAL OUTLOOK 2: Following resolution of current PTX DCB safety concerns, the present study supports evaluating paclitaxel DCBs as a regional endovascular therapy to stabilize atherosclerosis and improve long-term vascular outcomes in patients with PAD and coronary artery disease.

REFERENCES

1. Rosenfield K, Jaff MR, White CJ, et al. Trial of a paclitaxel-coated balloon for femoropopliteal artery disease. N Engl J Med 2015;373:145–53.

2. Scheinert D, Duda S, Zeller T, et al. The LEVANT i (lutonix paclitaxel-coated balloon for the prevention of femoropopliteal restenosis) trial for femoropopliteal revascularization: first-in-human randomized trial of low-dose drug-coated balloon versus uncoated balloon angioplasty. J Am Coll Cardiol Intv 2014;7:10–9.

3. Scheller B, Hehrlein C, Bocksch W, et al. Treatment of coronary in-stent restenosis with a paclitaxel-coated balloon catheter. N Engl J Med 2006;355:2113–24.

4. Jeger RV, Farah A, Ohlow M-A, et al. Drug-coated balloons for small coronary artery disease (BASKET-SMALL 2): an open-label randomised non-inferiority trial. Lancet 2018;392:849–56.

5. Feldman DN, Armstrong EJ, Aronow HD, et al. SCAI consensus guidelines for device selection in femoral-popliteal arterial interventions. Catheter Cardiovasc Interv 2018;92:124–40.

6. Katsanos K, Spiliopoulos S, Kitrou P, Krokidis M, Karnabatidis D. Risk of death following application of paclitaxel-coated balloons and stents in the femoropopliteal artery of the leg: a systematic review and meta-analysis of randomized controlled trials. J Am Heart Assoc 2018;7:e011245.

7. U.S. Food and Drug Administration. Treatment of peripheral arterial disease with paclitaxel-coated balloons and paclitaxel-eluting stents potentially associated with increased mortality - letter to health care providers. 06/20. Available at: https://www.fda.gov/medical-devices/letters-health-care-providers/update-treatment-peripheral-arterial-disease-paclitaxel-coated-balloons-and-paclitaxel-eluting. Accessed April 7, 2019.

8. Schneider PA, Laird JR, Doros G, et al. Mortality not correlated with paclitaxel exposure: an independent patient-level meta-analysis. J Am Coll Cardiol 2019;73:2550–63.

9. Secemsky EA, Kundi H, Weinberg I, et al. Association of survival with femoropopliteal artery revascularization with drug-coated devices. JAMA Cardiol 2019;4:332–40.

10. Secemsky EA, Kundi H, Weinberg I, et al. Drug-eluting stent implantation and long-term survival following peripheral artery revascularization. J Am Coll Cardiol 2019;73:2636–8.

11. Yoo H, Kim JW, Shishkov M, et al. Intra-arterial catheter for simultaneous microstructural and molecular imaging in vivo. Nat Med 2011;17:1680–4.

12. Hara T, Ughi GJ, McCarthy JR, et al. Intravascular fibrin molecular imaging improves the detection of unhealed stents assessed by optical coherence tomography in vivo. Eur Heart J 2017;38:447–55.

13. Stein-Merlob AF, Hara T, McCarthy JR, et al. Atheroma susceptible to thrombosis exhibit impaired endothelial permeability in vivo as assessed by nanoparticle-based fluorescence molecular imaging. Circ Cardiovasc Imaging 2017;10(5).

14. Phinikaridou A, Hallock KJ, Qiao Y, Hamilton JA. A robust rabbit model of human atherosclerosis and atherothrombosis. J Lipid Res 2009;50:787–97.

15. Schindelin J, Arganda-Carreras I, Frise E, et al. Fiji: an open-source platform for biological-image analysis. Nat Methods 2012;9:676–82.

16. Mintz GS, Nissen SE, Anderson WD, et al. American College of Cardiology Clinical expert consensus document on standards for acquisition, measurement and reporting of intravascular ultrasound studies (IVUS). A report of the American College of Cardiology Task Force on Clinical Expert Consensus Do. J Am Coll Cardiol 2001;37:1478–92.

17. Ughi GJ, Verjans J, Fard AM, et al. Dual modality intravascular optical coherence tomography (OCT) and near-infrared fluorescence (NIRF) imaging: a fully automated algorithm for the distance-calibration of NIRF signal intensity for quantitative molecular imaging. Int J Cardiovasc Imaging 2015;31:259–68.

18. Libby P, Ridker PM, Maseri A. Inflammation and atherosclerosis. Circulation 2002;105:1135–43.

19. Ridker PM, Everett BM, Thuren T, et al. Antiinflammatory Therapy with Canakinumab for Atherosclerotic Disease. N Engl J Med 2017;377:1119–31.

20. Liu C-L, Guo J, Zhang X, Sukhova GK, Libby P, Shi G-P. Cysteine protease cathepsins in cardiovascular disease: from basic research to clinical trials. Nat Rev Cardiol 2018;15:351–70.

21. Libby P, Ridker PM, Hansson GK. Progress and challenges in translating the biology of atherosclerosis. Nature 2011;473:317–25.

22. Wentzel JJ, Whelan DM, van der Giessen WJ, et al. Coronary stent implantation changes 3-D vessel geometry and 3-D shear stress distribution. J Biomech 2000;33:1287–95.

23. Calfon Press MA, Mallas G, Rosenthal A, et al. Everolimus-eluting stents stabilize plaque inflammation in vivo: assessment by intravascular fluorescence molecular imaging. Eur Heart J Cardiovasc Imaging 2017;18:510–8.

24. Cremers B, Schmitmeier S, Clever YP, Gershony G, Speck U, Scheller B. Inhibition of neointimal hyperplasia in porcine coronary arteries utilizing a novel paclitaxel-coated scoring balloon catheter. Catheter Cardiovasc Interv 2014;84:1089–98.

25. Cremers B, Milewski K, Clever YP, et al. Long-term effects on vascular healing of bare metal stents delivered via paclitaxel-coated balloons in the porcine model of restenosis. Catheter Cardiovasc Interv 2012;80:603–10.

26. Drachman DE, Edelman ER, Seifert P, et al. Neointimal thickening after stent delivery of paclitaxel: change in composition and arrest of growth over 6 months. J Am Coll Cardiol 2000;36:2325–32.

27. Verjans JW, Osborn EA, Ughi GJ, et al. Targeted near-infrared fluorescence imaging of atherosclerosis: clinical and intracoronary evaluation of indocyanine green. J Am Coll Cardiol Img 2016;9:1087–95.

28. Bozhko D, Osborn EA, Rosenthal A, et al. Quantitative intravascular biological fluorescence-ultrasound imaging of coronary and peripheral arteries in vivo. Eur Heart J Cardiovasc Imaging 2017;18:1253–61.

29. Ughi GJ, Wang H, Gerbaud E, et al. Clinical characterization of coronary atherosclerosis with dual-modality OCT and near-infrared autofluorescence imaging. J Am Coll Cardiol Img 2016;9:1304–14.

30. Whitley MJ, Cardona DM, Lazarides AL, et al. A mouse-human phase 1 co-clinical trial of a protease-activated fluorescent probe for imaging cancer. Sci Transl Med 2016;8:320ra4.

KEY WORDS atherosclerosis, drug-coated balloon, imaging, inflammation, peripheral arterial disease

APPENDIX For an expanded Methods section and supplemental tables and figures, please see the online version of this paper.